






Design and Optimization of an Adaptive Robotic Gripper using Finite Element Analysis and Generative Design

Richard Josiah C. Tan Ai¹ , Marcus Corso S. Pilapil² , Ryann Aldrich A. Shi³ , Jeruel Lawrence D. Badugas⁴  and Sted Micah T. Cheng⁵ 

¹De La Salle University, Manila, richard.tanai@dlsu.edu.ph

²De La Salle University, Manila, marcus_pilapil@dlsu.edu.ph

³De La Salle University, Manila, ryann_shi@dlsu.edu.ph

⁴De La Salle University, Manila, jeruel_badugas@dlsu.edu.ph

⁵De La Salle University, Manila, sted_cheng@dlsu.edu.ph

Corresponding author: Richard Josiah C. Tan Ai, richard.tanai@dlsu.edu.ph

Abstract. Various industries use robotic grippers. These grippers come in varied types and functions and protect workers' health and improve industries' growth. However, specialized grippers cannot adapt to complex materials; thus, they become a liability to these sectors in the long run. Adaptive grippers, a type of gripper, are not limited to specific object shapes. These tools can grasp objects of different shapes and sizes, thus showing a remarkable potential in various applications. Therefore, this study focused on designing a rigid body, two-finger adaptive robotic gripper and optimizing its mass without compromising its strength while maintaining a safety factor level of 2. The loading conditions for different types of grip sizes were formulated. The researchers gathered data from the related literature, integrated these inputs to design the gripper, simulated and optimized the gripper design using generative design, then validated the results by finite element analysis. Results show that the total mass of the gripper was reduced by 79% while maintaining a safety factor level of 2. These findings then indicate that the gripper has been successfully optimized and hint at the potential for better and lighter technologies to be developed in the future.

Keywords: Generative Design, Gripper, Topology Optimization

DOI: <https://doi.org/10.14733/cadaps.2023.44-55>

1 INTRODUCTION

According to a survey developed by UiPath and the Economist Intelligence Unit, more than 90% of organizations in Canada, France, Germany, India, Japan, Singapore, the United Kingdom, and the United States use technological advancements to automate their business processes [1]. Currently, automation has become such a trend that various organizations have started to adopt them in different sectors (e.g., aerospace, textile and leather, and food) to improve product manufacturing's

accuracy and consistency and increase workplace safety [2]. Technological advancements like robotic grippers are consistent with this trend. In fact, these tools possess strong gripping forces that are necessary to perform copious tasks with high accuracy and repeatability [3]. Robotic grippers vary from basic configurations, like parallel pneumatic grippers, to complex patterns, such as 3-Finger grippers. Similarly, grippers also vary depending on their usage. For instance, grabbing sheets require vacuum grippers, clenching flexible materials demand adhesive grippers, and many more. However, as much as these grippers benefit various industries, specialized grippers fall short when faced with materials of different shapes and sizes. In this regard, adaptive grippers, another gripper type that can be rigid- or soft-bodied, can showcase their remarkable capabilities by grasping/holding diverse ranges of objects that are suitable under different media [4], [5].

Because most studies in literature only focused on making specialized grippers without weight optimization, in this study, a rigid linkage type two-finger adaptive robotic gripper was designed, simulated, and optimized by the researchers. Eventually, the findings of this study will benefit the academic research community by providing new insights regarding the field of robotics, various industries by enhancing their production rates with more accuracy, and workers by increasing work safety.

2 REVIEW OF RELATED LITERATURE

Gripping and grasping have different processes which are achieved by different principles that are often observed and are often the topic of research in the industry. The grasping process consists of six fundamental steps, namely approaching (moving towards the object), coming into contact (either exposing the gripper's magnetic field to or touching the object), increasing the force (adjusting the gripper's strength to grab the object), securing (grabbing and preventing object slippage), moving (transferring the object to a desired location), and releasing (loosening the grip to liberate the object). These processes are important when looking into the overall performance of the gripper; therefore, improving and monitoring every step of the grasping process has been an interest of numerous studies [6]. Similarly, the stated processes are achieved through different principles that are aimed for different types of objects, wherein the most common type is exhibited by mechanical grippers that heavily rely on classical mechanics and often use two or four synchronously moving fingers – which makes it adjustable, adaptable, and viable to a wide range of environments. These principles can in fact be categorized into different prehension methods, namely the impactive method for rigid fingers, ingressive for the intrusive and non-intrusive grippers, astrictive for grippers that use vacuum adhesion, magnetic adhesion, and electroadhesion, and contiguous for thermal, chemical, and surface tension grippers [7].

In line with this study, mechanical grippers' simplicity in terms of design, adaptability in terms of the materials it can grip, and modularity in terms of parts, seem to be beneficial when researching adaptive grippers. In addition to this, because these grippers obey the classical Newtonian mechanics, it is less difficult to test, predict, control, and limit the designed prototypes since there are many software simulations that can easily simulate and record changes done to such grippers – which makes optimization a lot easier. Furthermore, when studying the performance of the gripper and its finger, monitoring steps (ii.), (iii.), and (iv.) of the gripping process is critical.

Robotic grippers have driven industrialization in diverse industries like aerospace, textile and leather, and food. Examples of their respective uses in the said fields include producing dry carbon parts [8], weaving fabrics [9], handling goods [10], and many more. Currently, manufacturing techniques in most industries involve manual and sophisticated methodologies, small batch sizes, numerous variants, and material characteristics that are difficult to deal with. Hence, to overcome these limitations in the field of manufacturing, academic researchers have shifted to concentrate on applying automation as an alternative for the aforementioned techniques and enhancing process chain reliability [6].

Technological advancements have steered grippers' development, making their progress evident in the current generation. With the rise of such breakthroughs, new findings from different studies

have also naturally emerged and become trends in this field. In fact, the main goal of these recent studies is to enhance the gripper by manipulating its mechanisms and structures without compromising its performance. Examples include enhancing adaptive grippers' grasping abilities by increasing their contact points and surface area [6], lowering the number of actuators to improve gripper control [11], and many more. Indeed, through these emerging trends, gripper technology has become better and more efficient than ever before.

The adaptive gripper mechanism's designs can be categorized into three main gripping techniques, namely gripping by controlled (i.) adhesion, (ii.) stiffness, and (iii.) actuation. First, gripping by controlled adhesion involves an interaction between two surfaces that is controlled in various ways to generate a force (e.g., friction) strong enough to grip an object. Second, gripping by controlled stiffness entails two gripping stages. The soft stage occurs when the gripper approaches and encompasses the object, while the stiff stage follows as the gripper grasps/grips it. Because there are a vast number of gripping principles, different means can be used in this technique. Lastly, gripping by actuation is seemingly the most utilized technique in most studies as it heavily relies on the fingers that are controlled by passive or active actuators [12].

Since actuated grippers achieve adaptability by changing their finger design, numerous works have surfaced to share insights about different gripper designs. The gripper of [13] grasps and encompasses objects of different shapes by using the "Fin ray" effect; however, some researchers still favor rigidly designed grippers due to their robustness and predictability. The universal gripper design of Harada et al [14] showcases a combination of both soft and rigid components. The design consists of four actuated fingers for gripping: two are passive fingers for object orienting, while the other two are actuated fingers for gripping. The design of Furata et al. [15] consists of two rigid fingers (for pinching), with one passively actuated joint each, wherein every finger base is connected to a motorized actuator. The design of Liu et al [16] only includes four rigid fingers actuated by a rotating motor in the middle, which is connected to a screw that opens and closes the fingers. The design of [17] consists of two fingers that possess the ability to encompass and pinch and exhibit great modularity and easy programmable software. The design of Birglen [18] closely resembles that of [13] in which the gripper consists of two parallel fingers that have passively actuated pin joints, which connects to two phalanges at each front and back portion of the finger. The design of [5] is similar to [18], except the back portion. Instead of making it pin-jointed, the back portion design of each finger is rigid, thereby improving predictability.

To be able to grip more shapes and sizes of objects, some gripper designs employ multiple modes of grasping. Bai et al [19] synthesized a gripper a meso-gripper, in which can grip objects in the mesoscopic scale. The gripper features two gripping modes the passive adjusting for larger objects and angled gripping modes for smaller objects. The gripper is designed to grasp objects with sizes from 0.5mm to 100mm. Hao et al [20] designs a multimode compliant gripper using the singularities of the four-bar mechanism. The mobility of the compliant gripper can be reconfigurable to grasp a variety of shapes, this motion is controlled by two actuators at the base of the gripper. The gripper can produce parallel actuation and angled actuation. Depending on the task, various modes of actuation can be used to efficiently grip the object. Backus and Dollar [21] designed a gripper designed for ungrounded vehicles such as aerial drones. They designed a three-finger gripper, which uses prismatic proximal followed by a revolute distal joint and is actuated by a single motor and tendon based underactuated transmission. The design of Kok [5] used multiple gripping modes, which is the pinching and encompassing but only has one actuation motion, the two types of gripping modes are achieved based on where the object contacts the gripper.

To optimize the gripper finite element analysis will be used to validate the design. Stiffness and weight are the important parameter in this application. Brassitos and Jalili [22] designed a compact high-torque robotic actuator for space mechanisms. They optimized the joint drive system of a specific robot in which it would give maximum torque density for its size. This was done by numerical analysis by establishing boundary conditions and performing finite element analysis to compute the maximum stresses.

Overall, the mechanism of gripping by actuation promises reliability, controllability, and predictability when developing adaptive end-effectors. Because the actuated grippers' adaptability is heavily reliant on the fingers of the gripper, most researchers focus on the development of these fingers whenever creating an adaptive gripper design. Moreover, as seen from the examples above, designs concerning the combination between rigid and soft parts have been developed; however, such blueprints seem to lessen the predictability of the product while adding unwanted limitations to its applicability. In this regard, fully rigid grippers are favored due to their robustness, predictability, and consistency in performance. Furthermore, when choosing between fully and passively actuated mechanisms, it seems that passively actuated parallel grippers show more promising results because there are fewer limitations in the opening size. Also, having a two-fingered gripper is beneficial due to its ability to grip more irregularly shaped objects.

Designing, simulating, and optimizing the adaptive gripper is the main objective of this research study. In line with this, the following needs to be accomplished:

1. To design an optimized rigid body, two-finger adaptive robotic gripper, with similar kinematics with Kok et al [5], that accommodates various grip sizes and forces
2. To formulate the loading condition for different pinch and grasp sizes
3. To optimize the designed gripper's mass without compromising its strength while conforming to a minimum factor of safety (FoS) level of 2
4. (To validate the results by simulating the gripper performance under different loading conditions and comparing it to the baseline design using Finite Element Analysis

3 METHODOLOGY

The researchers initially analyzed the design of Kok et al [5]. It is modeled in a CAD software and the grasp scenarios for a cylindrical object that were introduced in the paper are analyzed. The gripper consists of two fingers which are actuated with a prismatic joint towards each other. The finger is a four-bar linkage, which is assisted by a spring to return to its starting position. The mode of grasping depends on how the gripper contacts the object. The three grasping modes, each with unique loading conditions, are shown in Figure 1. The first mode is the pinch, where object is grasped with a parallel-forces, this occurs when the object is gripped by the tip of the gripper above two pins connecting the tip. The second mode is the encompassing grasp for smaller objects, wherein the upper and lower phalanx applies a contact force to the object. The tip of the two fingers pushes against each other and this provides the force on the upper and lower phalanx on transmission. The third mode is the encompassing grasp for large objects, this position occurs when encompassing objects with diameter of 50 mm or more. At this mode, the back of the upper phalanx is in contact with the base and this fixes the position of the linkages.

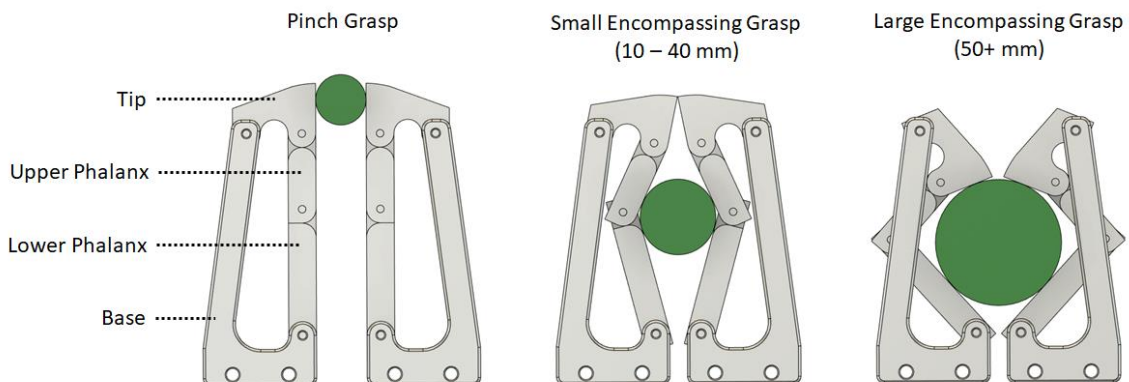


Figure 1: Three Gripping Modes (a) Pinch (b) Small Encompassing (c) Large Encompassing.

To be able to optimize each part of the gripper using generative design the loading conditions (boundary conditions) for each part has to be identified. The loading condition for Pinch, Small Encompassing (10 – 40 mm) and Large Encompassing (50 mm) will be computed. Forces on the joints, external forces and contact forces will be computed. In both pinching and encompassing grasps, the gripper exerts 100 N as it moves towards the cylindrical object with a known diameter for grasping. The equations for each grasp condition for each component are formulated. These equations are then solved as systems of linear equations. The forces obtained from the solution will be used as boundary condition for the generative design and finite element analysis.

The forces for the pinch grasp are shown in Figure 2. In this figure a force at point E is provided by the actuator, at the tip force G_0 is given by the contact force with the object that is gripped.

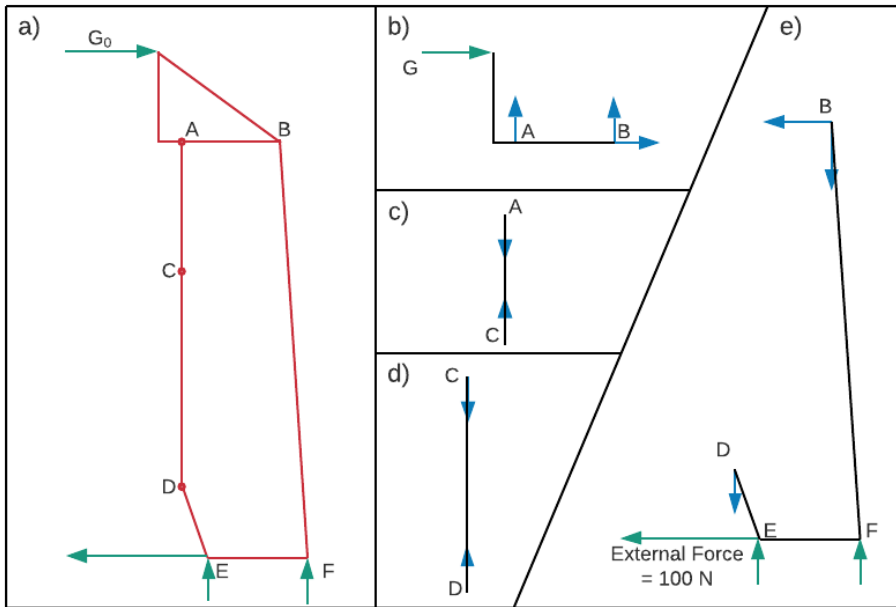


Figure 2: Pinch grasp loading conditions.

From Figure 2, the summation of forces and summation of moment equations can be derived. The equations are shown in Equations (1 to 8).

$$\Sigma F_{x-T} = B_x + G_0 = 0 \quad (1)$$

$$\Sigma F_{y-T} = A_y + B_y = 0 \quad (2)$$

$$\Sigma M_A = \overline{AB}_x \cdot B_y - \overline{GA}_y \cdot G_0 = 0 \quad (3)$$

$$\Sigma F_{y-U} = -A_y + C_y = 0 \quad (4)$$

$$\Sigma F_{y-L} = -C_y + D_y = 0 \quad (5)$$

$$\Sigma F_{x-B} = -B_x = 100 \quad (6)$$

$$\Sigma F_{y-B} = -B_y - D_y + E_y + F_y = 0 \quad (7)$$

$$\Sigma M_E = \overline{DE}_y \cdot D_x + \overline{DE}_x \cdot D_y + \overline{FE}_x \cdot F_y + \overline{BE}_y \cdot B_x - \overline{BE}_x \cdot B_y = 0 \quad (8)$$

The encompassing grasp of the 10mm - 40mm cylindrical object is shown in Figure 3. As seen in the figure, the object is grasped by the gripper while exerting normal forces H and I on the upper and lower phalanxes, respectively. Likewise, force G is present at point G because the two tips of the gripper would push against each other. Conversely, the encompassing grasp of the 50mm cylindrical object (with a maximum angle of 42.3 degrees in reference to the positive y-axis at point D) is

shown in Figure 4. As seen in the figure, normal forces G and I result from grasping the object. Moreover, it is also observed that a cylindrical stopper is placed to ensure that the gripper can hold the object firmly, resulting in a contact force H that is perpendicular to the upper phalanx.

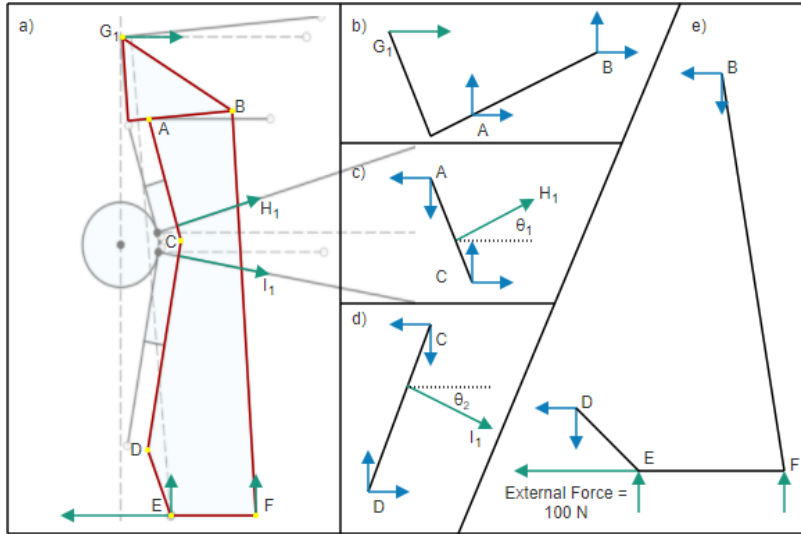


Figure 3: Encompassing grasp loading conditions for cylindrical object with 10mm - 40mm diameter, (a) The sketch of the whole gripper with net forces present and the free-body diagrams of the (b) tip, (c) upper phalanx, (d) lower phalanx, and (e).

For the encompassing grasp of the 10mm - 40mm cylindrical object, Equations 9 to 20 show the summation of forces in x and y and summation of moments in each of the four components: the tip, upper phalanx, lower phalanx, and base. Moreover, the gripper is simplified to its critical points, points A to G (indicated by yellow dots), and analyzed through the method of joints. Equation 21 shows the relationship of the contact force assuming that the cylinder is well gripped.

$$\Sigma F_{x-T} = A_x + B_x + G_1 = 0 \quad (9)$$

$$\Sigma F_{y-T} = A_y + B_y = 0 \quad (10)$$

$$\Sigma M_A = -\overline{AB}_y \cdot B_x + \overline{AB}_x \cdot B_y - \overline{GA}_y \cdot G_1 = 0 \quad (11)$$

$$\Sigma F_{x-U} = -A_x + C_x + H_1 \cos \theta_1 = 0 \quad (12)$$

$$\Sigma F_{y-U} = -A_y + C_y + H_1 \sin \theta_1 = 0 \quad (13)$$

$$\Sigma M_C = \overline{AC}_y \cdot A_x + \overline{AC}_x \cdot A_y - \overline{HC} \cdot H_1 = 0 \quad (14)$$

$$\Sigma F_{x-L} = -C_x + D_x + I_1 \cos \theta_2 = 0 \quad (15)$$

$$\Sigma F_{y-L} = -C_y + D_y - I_1 \sin \theta_2 = 0 \quad (16)$$

$$\Sigma M_D = \overline{CD}_y \cdot C_x - \overline{CD}_x \cdot C_y - \overline{ID} \cdot I_1 = 0 \quad (17)$$

$$\Sigma F_{x-B} = -B_x - D_x = 100 \quad (18)$$

$$\Sigma F_{y-B} = -B_y - D_y + E_y + F_y = 0 \quad (19)$$

$$\Sigma M_E = \overline{DE}_y \cdot D_x + \overline{DE}_x \cdot D_y + \overline{FE}_x \cdot F_y + \overline{BE}_y \cdot B_x - \overline{BE}_x \cdot B_y = 0 \quad (20)$$

$$H_1 \sin \theta_1 - I_1 \sin \theta_2 = 0 \quad (21)$$

For the Large Encompassing Grasp that is for objects with diameter of 50 mm and above, the forces on the components are shown on Figure 4. This is the maximum position of the gripper and the upper phalanx contacts with the base. This provides the force H_2 on the upper phalanx.

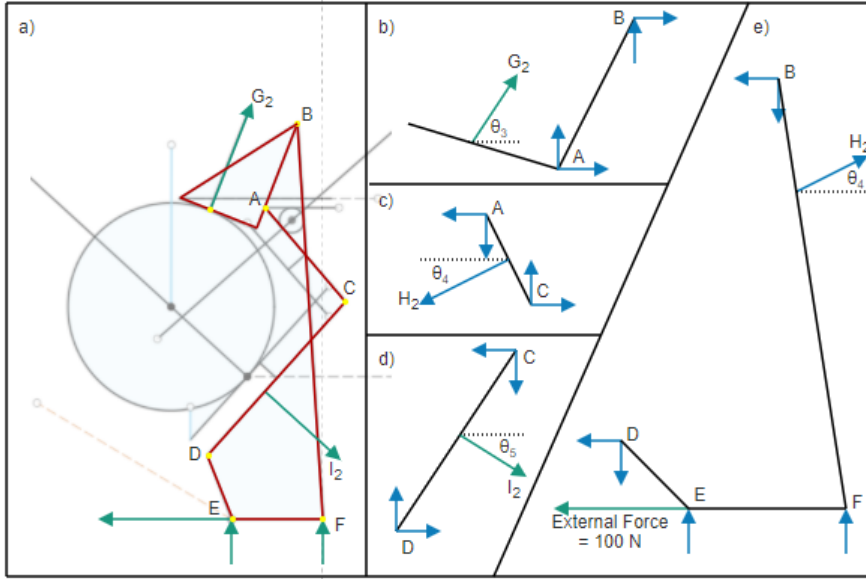


Figure 4: Encompassing grasp loading conditions for cylindrical object with 50mm diameter, (a) The sketch of the whole gripper with net forces present and the free-body diagrams of the (b) tip, (c) upper phalanx, (d) lower phalanx, and (e) base.

In terms of the set of equations used, the 50mm setup is different compared to that of the 10mm - 40mm because point B is above point G, thus the loading condition will be different. Therefore, a different set of equations (Equations 14 to 26) is used to obtain the force values.

$$\Sigma F_{x-T} = A_x + B_x + G_2 \cos \theta_3 = 0 \quad (22)$$

$$\Sigma F_{y-T} = A_y + B_y + G_2 \sin \theta_3 = 0 \quad (23)$$

$$\Sigma M_A = -\overline{AB}_y \cdot B_x + \overline{AB}_x \cdot B_y - \overline{GA} \cdot G_2 = 0 \quad (24)$$

$$\Sigma F_{x-U} = -A_x + C_x - H_2 \cos \theta_4 = 0 \quad (25)$$

$$\Sigma F_{y-U} = -A_y + C_y - H_2 \sin \theta_4 = 0 \quad (26)$$

$$\Sigma M_C = \overline{AC}_y \cdot A_x + \overline{AC}_x \cdot A_y - \overline{HC} \cdot H_2 = 0 \quad (27)$$

$$\Sigma F_{x-L} = -C_x + D_x + I_2 \cos \theta_5 = 0 \quad (28)$$

$$\Sigma F_{y-L} = -C_y + D_y - I_2 \sin \theta_5 = 0 \quad (29)$$

$$\Sigma M_D = \overline{CD}_y \cdot C_x - \overline{CD}_x \cdot C_y - \overline{ID} \cdot I_2 = 0 \quad (30)$$

$$\Sigma F_{x-B} = -B_x - D_x + H_2 \cos \theta_4 = 100 \quad (31)$$

$$\Sigma F_{y-B} = -B_y - D_y + E_y + F_y + H_2 \sin \theta_4 = 0 \quad (32)$$

$$\Sigma M_E = \overline{DE}_y \cdot D_x + \overline{DE}_x \cdot D_y + \overline{FE}_x \cdot F_y + \overline{BE}_y \cdot B_x - \overline{BE}_x \cdot B_y - \overline{HE} \cdot H = 0 \quad (33)$$

$$G_2 \sin \theta_3 - I_2 \sin \theta_5 = 0 \quad (34)$$

Where:

$\Sigma F_{x-T}, \Sigma F_{x-U}, \Sigma F_{x-L}, \Sigma F_{x-B}$ = total forces along the x-axis of the tip, upper phalanx, lower phalanx, and base, respectively.

$\Sigma F_{y-T}, \Sigma F_{y-U}, \Sigma F_{y-L}, \Sigma F_{y-B}$ = total forces along the y-axis of the tip, upper phalanx, lower phalanx, and base, respectively.

$\Sigma M_A, \Sigma M_C, \Sigma M_D, \Sigma M_E$ = total moments around points A, C, D, and E, respectively.

A_x, B_x, C_x, D_x = horizontal forces experienced by points A, B, C, and D, respectively.

$A_y, B_y, C_y, D_y, E_y, F_y$ = vertical forces experienced by points A, B, C, D, E, and F, respectively.

G_0, G_1, G_2 = horizontal force exerted at the tip for Pinch, Small Encompassing, Large Encompassing.

H_1, H_2 = normal forces exerted at the upper phalanx (in Figure 3 and Figure 4, respectively).

I_1, I_2 = normal forces exerted at the lower phalanx (in Figure 3 and Figure 4, respectively).

$\theta_1, \theta_2, \theta_3, \theta_4, \theta_5$ = reference angles of force $H_1, I_1, G_2, H_2,$ and $I_2,$ respectively.

$\overline{AB}_x, \overline{AC}_x, \overline{BE}_x, \overline{CD}_x, \overline{DE}_x, \overline{FE}_x$ = horizontal distances between points A and B, A and C, B and E, C and D, D and E, and F and E, respectively.

$\overline{AB}_y, \overline{AC}_y, \overline{BE}_y, \overline{CD}_y, \overline{DE}_y, \overline{GA}_y$ = vertical distances between points A and B, A and C, B and E, C, and D, D and E, and G and C, respectively.

$\overline{GA}, \overline{HC}, \overline{ID}$ = distances between points G and A, H and C, and I and D, respectively.

The calculated the forces on each component for all of the grasp modes are used as the boundary condition for generative design. Autodesk Fusion 360 Generative Design allows the user to define constraints, materials, manufacturing method and target objective in which it will generate proposals for the part. For the setup, Aluminum alloy (AlSi10Mg) is used as the study material and the manufacturing method is limited to additive manufacturing. It has the following mechanical properties: Young's Modulus of 71 GPa, Poisson's Ratio of 0.33, Yield Strength of 240 MPa, and Ultimate Tensile Strength of 460 MPa. Following this, gripper simulation (using a mesh parameter size of 3%) and optimization were simultaneously conducted. Each part is optimized individually, each part has six loading conditions to satisfy, the pinch and the encompassing grasps for 10, 20, 30, 40, 50mm. The objective target is set to minimize mass while complying to a Factor of Safety (FoS) of 2. This is calculated from the maximum von Mises Stress (vMS) of the object in relation to the yield strength of the material used. Generative Design requires the user to indicate the preserve geometry, starting geometry and obstacle geometry. The preserve geometry is the surface around the holes in the pin joints and the flat surfaces where the object to grip physically contacts. The starting geometry is the original part. The obstacle geometry includes planes, cylinders and features to prevent the model from filling the holes in the pins and obstructing the contact surface with the objects. After solving for the solution for the generative design. From the set of generated solids, the one with the best strength to mass ratio is selected. After obtaining the result of the generative design, some adjustments are made to preserve symmetry.

To validate the results of the generative design, a static stress analysis on the gripper parts using the boundary conditions was conducted. The results of original and optimized design which yields the lowest FoS are compared to each other. To further assess the results of the generative design, a static stress analysis on the optimized gripper assembly using the external force as boundary conditions was conducted.

4 RESULTS AND DISCUSSION

The results of the stress simulation for each component is shown in Table 1. The FoS of the original design has a FoS greater than 15 except for the Base which has a factor of safety of 14.78 which is still way beyond what is needed for the task. For the optimized design, the minimum FoS of the parts is 2.336 which is in the upper phalanx. For the reduction in mass, the optimized tip, upper phalanx, lower phalanx, and base have a significant mass reduction of 83%, 90%, 91%, and 69%, respectively. This reduces the mass of the entire gripper assembly by 79%, while still conforming to a FoS of 2.

Part	Minimum FoS			Mass (kg)		
	Original	Optimized	%Change	Original	Optimized	%Change
Tip	15+	5.496	63%	0.030	0.005	83%
Upper Phalanx	15+	2.336	84%	0.020	0.002	90%
Lower Phalanx	15+	2.459	84%	0.034	0.003	91%
Base	14.78	6.069	59%	0.084	0.026	69%
Total	-	-	-	0.168	0.036	79%

Table 1: The original and optimized grippers' minimum FoS and mass (kg).

The actual loading of the system for an assembly is more complex, thus the stress for each component when tested as an assembly is different. The results for the static stress analysis for all the loading conditions for the optimized gripper assembly is shown in Figure 5.

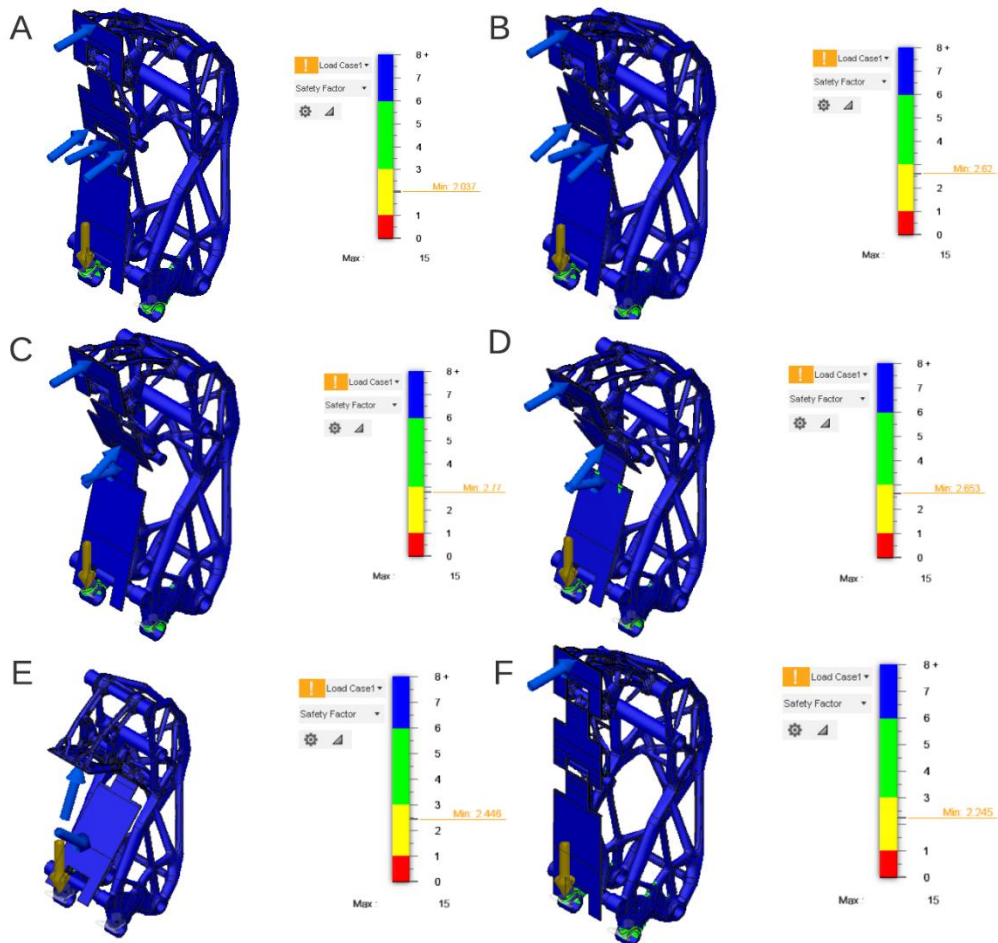


Figure 5: Simulation results of the optimized gripper design at 100N for different loading conditions (A) 10mm, (B) 20mm, (C) 30mm, (D) 40mm, (E) 50mm, and (F) pinch.

Figure 6 and Figure 7 showcase the differences between the original and optimized gripper designs. Although significant reduction in mass is achieved by the optimization, the total bounding volume consumed by the gripper increases. It is also shown that the optimized gripper is a more organic design and shows similarity to the shape of a claw of a crab or lobster.

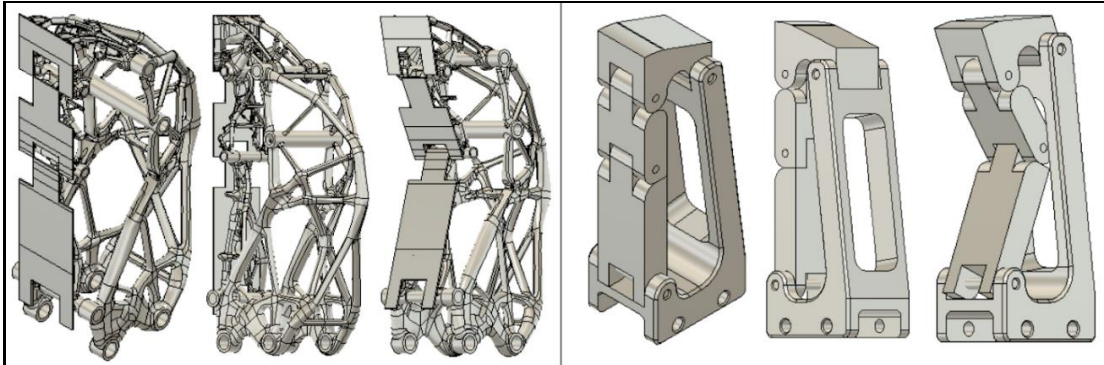


Figure 6: The assembled optimized (left) vs. original (right) gripper designs.

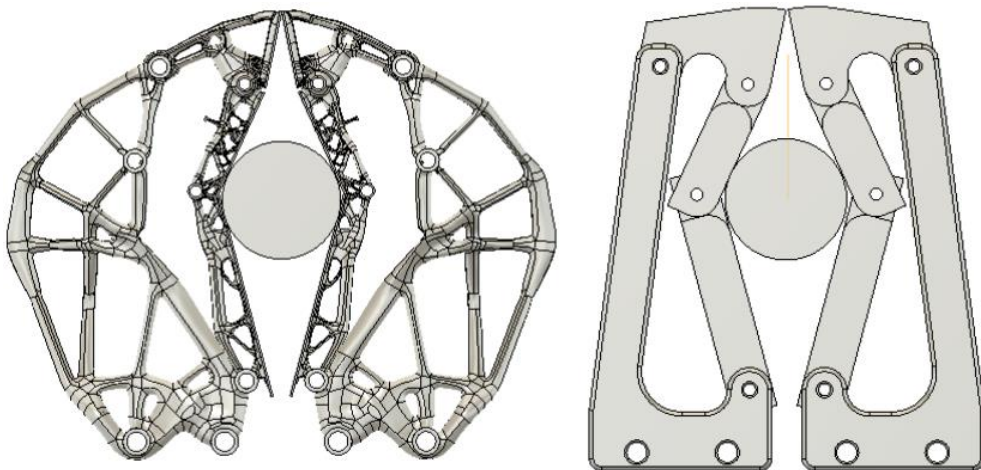


Figure 7. Visualizing the encompassing grasp of optimized (left) and original (right) gripper designs.

5 CONCLUSION AND RECOMMENDATION

Through the remarkable capabilities of Generative Design, the researchers successfully optimized an adaptive robotic gripper by reducing its total mass (about 79%) without compromising its strength while maintaining an FoS level of 2. Likewise, results from this study feature a lighter gripper, resulting in a greater possible payload for the machine or robot to utilize. More importantly, the findings of this study could hint at the possibility of better and lighter technologies that can be developed in the near future. That said, the broad scope and abilities of generative design, together with the application of the principles from this study, can be applied to other industries.

Since only five load cases for a cylindrical material were considered in this study, future researchers could also add more load cases and shapes or go beyond the simulation workspace by fabricating the and testing the gripper. Consistently, future studies can also include variables like torsional spring for returning the gripper to the original position and gripper arm and actuator to

test the performance of the gripper in actual grasping. For applications with less control on the external forces applied to the gripper the safety factor could be increased to accommodate for this variability. Furthermore, the current load case only considers a static force from the gripper, in future studies the actuation method and impulse from the impact of the gripper could be used to set the forces of the boundary condition for the generative design.

Richard Josiah C. Tan Ai, <https://orcid.org/0000-0003-2585-1912>

Marcus Corso S. Pilapil, <https://orcid.org/0000-0002-6644-4515>

Ryann Aldrich A. Shi, <https://orcid.org/0000-0002-8952-0904>

Jeruel Lawrence D. Badugas, <https://orcid.org/0000-0002-2856-4815>

Sted Micah T. Cheng, <https://orcid.org/0000-0001-6896-0890>

REFERENCES

- [1] New study shows adoption of business automation technologies is driven by the c-suite. <https://www.businesswire.com/news/home/20190625005333/en/New->
- [2] Granta: Advantages and disadvantages of automation, 2017. <https://www.granta-automation.co.uk/news/advantages-and-disadvantages-of-automation/>
- [3] Chang, J.Y.: Adaptive robotic gripper: The pathway to industrial revolution 4.0 and smart manufacturing, Open access government, 2019. <https://www.openaccessgovernment.org/smart-engineering/67019/>.
- [4] Bélanger-Barrette, M.: Top 4 reasons to use an adaptive electric gripper, 2014. <https://blog.robotiq.com/bid/72618/Top-4-Reasons-to-Use-an-Adaptive-Electric-Gripper>.
- [5] Kok, Y.Y.: Design of an adaptive finger with encompassing grasp capability for parallel grippers, 2019. <http://doi.org/10.32657/10220/49336>.
- [6] Fantoni, G.; Santochi, M.; Dini, G.; Tracht, K.; Scholz-Reiter, B.; Fleischer, J.; Kristoffer Lien, T.; Seliger, G.; Reinhart, G.; Franke, J.; Nrgaard Hansen, H.; Verl, A.: Grasping devices and methods in automated production processes, CIRP Annals, 63(2), 679–701, 2014. <http://doi.org/10.1016/j.cirp.2014.05.006>.
- [7] Monkman, G.J.; Hesse, S.; Steinmann, R.; Schunk, H.: Robot grippers, Wiley, 2007. ISBN 978-3-527-60989-5.
- [8] Angerer, A.; Ehinger, C.; Hoffmann, A.; Reif, W.; Reinhart, G.; Strasser, G.: Automated cutting and handling of carbon fiber fabrics in aerospace industries, 2010 IEEE International Conference on Automation Science and Engineering, 2010. ISSN 9781424454471. <http://doi.org/10.1109/coase.2010.5584262>.
- [9] Seliger, G.; Szimmat, F.; Niemeier, J.; Stephan, J.: Automated handling of non-rigid parts, CIRP Annals, 52(1), 21–24, 2003. [http://doi.org/10.1016/s0007-8506\(07\)60521-6](http://doi.org/10.1016/s0007-8506(07)60521-6).
- [10] Blanes, C.; Mellado, M.; Beltran, P.: Novel additive manufacturing pneumatic actuators and mechanisms for food handling grippers, Actuators, 3(3), 205–225, 2014. <http://doi.org/10.3390/act3030205>.
- [11] Dollar, A.M.; Howe, R.D.: The highly adaptive SDM hand: Design and performance evaluation, The International Journal of Robotics Research, 29(5), 585–597, 2010. <http://doi.org/10.1177/0278364909360852>.
- [12] Shintake, J.; Cacucciolo, V.; Floreano, D.; Shea, H.: Soft robotic grippers, Advanced Materials, 30(29), 1707035, 2018. <http://doi.org/10.1002/adma.201707035>.
- [13] Festo: Adaptive gripper fingers DHAS, 2017. https://www.festo.com/cat/en-gb_gb/data/doc_ENGB/PDF/EN/DHAS_EN.PDF.
- [14] Harada, K.; Nagata, K.; Rojas, J.; Ramirez-Alpizar, I.G.; Wan, W.; Onda, H.; Tsuji, T.: Proposal of a shape adaptive gripper for robotic assembly tasks, Advanced Robotics, 30(17-18), 1186–1198, 2016. <http://doi.org/10.1080/01691864.2016.1209431>.
- [15] Furata, Y.; Tsuji, T.; Suzuki, Y.; Watanabe, T.; Hikizu, M.; Seki, H.: Adaptive gripper with soft sheets for a uniformly distributed grasping force, 2017 IEEE International Conference on

- Robotics and Biomimetics (ROBIO), 2017. ISSN 9781538637425. <http://doi.org/10.1109/robio.2017.8324446>.
- [16] Liu, C.; Cheng, J.; Li, Z.; Cheng, C.; Zhang, C.; Zhang, Y.; Zhong, R.Y.: Design of a self-adaptive gripper with rigid fingers for Industrial Internet, Robotics and Computer-Integrated Manufacturing, 65, 101976, 2020. <http://doi.org/10.1016/j.rcim.2020.101976>.
- [17] Robotiq: 2F-85 and 2F-140 grippers, 2020. <https://robotiq.com/products/2f85-140-adaptive-robot-gripper>.
- [18] Birglen, L.: Enhancing versatility and safety of industrial grippers with adaptive robotic fingers, 2015 IEEE/RSJ International Conference on Intelligent Robots and Systems (IROS), 2015. ISSN 9781479999941. <http://doi.org/10.1109/iros.2015.7353778>.
- [19] Bai, G.; Kong, X.; Ritchie, J.M.: Kinematic analysis and dimensional synthesis of a meso-gripper, Journal of Mechanisms and Robotics, 9(3), 1–13, 2017. ISSN 19424310. <http://doi.org/10.1115/1.4035800>.
- [20] Hao, G.; Li, H.; Nayak, A.; Caro, S.: Design of a compliant gripper with multimode jaws, Journal of Mechanisms and Robotics, 10(3), 2018. ISSN 1942-4302. <http://doi.org/10.1115/1.4039498>.
- [21] Backus, S.B.; Dollar, A.M.: A prismatic-revolute-revolute joint hand for grasping from unmanned aerial vehicles and other minimally Constrained Vehicles, Journal of Mechanisms and Robotics, 10(2), 1–8, 2018. ISSN 19424310. <http://doi.org/10.1115/1.4038975>.
- [22] Brassitos, E.; Jalili, N.: Design and development of a compact high-torque robotic actuator for space mechanisms, Journal of Mechanisms and Robotics, 9(6), 1–11, 2017. ISSN 1942-4302. <http://doi.org/10.1115/1.4037567>.